Geo-Mar Lett (2010) 30:1–13
DOI 10.1007/s00367-009-0145-7

ORIGINAL

Calcareous nannofossil and planktonic foraminiferal distributional patterns during deposition of sapropels S6, S5 and S1 in the Libyan Sea (Eastern Mediterranean)

Maria V. Triantaphyllou · Assimina Antonarakou · Margarita Dimiza · Christos Anagnostou

Received: 4 February 2009 / Accepted: 29 June 2009 / Published online: 17 July 2009

Abstract In core ADE3-23 collected in the Libyan Sea, the nannofossil species *Coccolithus pelagicus*, *Coronosphaera* spp., *Helicosphaera* spp., *Syracosphaera* spp., *Calcidiscus* spp., small *Gephyrocapsa* spp., and the planktonic foraminifers *Globigerina bulloides*, *Neogloboquadrina pachyderma*, *Globorotalia scitula*, *Turborotalita quinqueloba* and *Neogloboquadrina dutertrei* prevail in sapropel S6 (midpoint at 172 ka B.P.), indicative of cold and highly productive surface conditions. Warm and highly stratified water-column conditions are recorded by the characteristic assemblage of *Globigerinoides ruber*, *Globoturborotalita rubescens*, *Florisphaera profunda*, *Rhabdosphaera* spp. during the sapropel S5 depositional interval (midpoint at 124 ka B.P.). Compared with S5, *Globigerinita glutinata*, *Globorotalia inflata*, *Globigerinella siphonifera*, *Globorotalia truncatulinoides* and the calcareous nannofossil *Emiliania huxleyi* characterise less stratified conditions within sapropel S1 (midpoint at 8.5 ka B.P.). Multivariate statistical analyses of calcareous nannofossil and planktonic foraminifers in core ADE3-23 identify planktonic assemblages which typify sapropels S6, S5 and S1 in the Libyan Sea. A warmer interval is recognised in the middle part of the cold S6, and can be associated with an influx of less saline waters and the occurrence of a faint, temporary deep chlorophyll maximum. Evidence for enhanced surface productivity and breakdown of stratification is observed in the middle–upper part of the warm S5, associated with climatic deterioration. Moreover, an increase in surface productivity in the upper S1 implies weak stratification. Our combined calcareous nannofossil and planktonic foraminiferal data add to the evidence that climate variability was more pronounced than commonly considered to date for all the three studied Eastern Mediterranean sapropel depositional intervals.

M. V. Triantaphyllou (✉) · A. Antonarakou · M. Dimiza
Faculty of Geology & Geoenvironment, Department of Historical Geology-Palaeontology, University of Athens,
Panepistimiopolis,
15784 Athens, Greece
e-mail: mtriant@geol.uoa.gr

C. Anagnostou
Institute of Oceanography, Hellenic Centre for Marine Research,
P.O. Box 712,
19013 Anavissos, Greece

Introduction

Though the Eastern Mediterranean is generally characterised by low primary productivity (e.g. Psarra et al. 2000) and organic-poor sediments, the late Pleistocene deposition of sapropels (dark-coloured organic-rich sedimentary layers) demonstrates that dramatically different conditions periodically occurred and coincided with changes in global and regional climate (Cita et al. 1977; Vergnaud-Grazzini et al. 1977). The precessional minima with which sapropels coincide are periods of more humid climate in the Mediterranean (e.g. Rohling and Hilgen 1991; Lourens et al. 1992), associated with increased river runoff and higher delivery of soil-derived nutrients, thereby promoting primary production. The high content of organic carbon in the sapropels implies a combination of elevated marine productivity and enhanced preservation of organic matter under deep-water anoxic conditions (e.g. Bethoux et al. 1999; de Lange et al. 1999). Enhanced burial of organic carbon in sediments was likely initiated by an influx of low-salinity waters which slowed or halted convective overturning in the Eastern Mediterranean and reduced deep-water oxygenation (e.g. Rohling and Gieskes 1989; Emeis et al. 2000a). Recent palaeoceanographic records suggest that, during intervals of precession minima, the

Eastern Mediterranean climate was less stable than previously thought (e.g. Rohling et al. 2002a, 2004; Casford et al. 2003; Gogou et al. 2007; Marino 2008).

Numerous studies have revealed the dynamics of planktonic communities during sapropel deposition in the Eastern Mediterranean (among others, Violanti et al. 1991; Castradori 1993a, 1993b; Capotondi et al. 1999; Negri et al. 1999; Geraga et al. 2000, 2005; Negri and Giunta 2001; Cane et al. 2002; Corselli et al. 2002; Giunta et al. 2003, 2006; Principato et al. 2003, 2006; Triantaphyllou et al. 2009). However, few of these (e.g. Negri et al. 1999; Corselli et al. 2002) have compared different sapropel layers in terms of abundance and identity of both calcareous nannofossils and planktonic foraminifers.

In this work, we have performed calcareous nannofossil and planktonic foraminiferal analyses in sediments of core ADE3-23 collected in the Libyan Sea, and have assessed comparative distributional patterns in order to identify ecological affinities of calcareous plankton assemblages within sapropels S6, S5 and S1. We aim at contributing to existing evidence of climatic instability during sapropel deposition in the Eastern Mediterranean.

Physical setting

The modern Mediterranean Sea is characterised by an anti-estuarine circulation pattern driven by wind stress and thermohaline forcing (POEM Group 1992). The inflow of Atlantic surface water and the deep-water outflow contribute to its oligotrophic nature, as more nutrients are exported to than received from the Atlantic Ocean (Bethoux et al. 1999). Nutrient-depleted Modified Atlantic Water enters the Mediterranean Sea through the Strait of Gibraltar, and becomes gradually saltier and warmer to balance evaporation while it flows eastwards (e.g. Pinardi and Masetti 2000). Modified Atlantic Water enters the Eastern Mediterranean through the Strait of Sicily, with high salinities. It feeds the Ionian Current and Mid-Mediterranean Jet through the Ionian Sea and the Levantine Basin respectively (Fig. 1). This circulation features several small-scale cyclonic and anticyclonic gyres and eddies which change intensity and location, due to atmospheric forcings (Pinardi and Masetti 2000) and the irregular topographic structure of the basin (POEM Group 1992). Seasonal density variability of surface waters causes the formation of the Eastern Mediterranean Deep Water, as well as the Levantine Intermediate Water which forms in the Rhodes gyre region in the northwest Levantine Basin, by vertical mixing during winter (Malanotte-Rizzoli et al. 1997).

In the Libyan Sea, circulation of surface water is modulated by the effect of one cyclonic gyre, the Cretan gyre (Karageorgis et al. 2008). This part of the Eastern Mediterranean Sea is also affected by the arid conditions of northern Africa, the Arabian Peninsula and the Near East. Fluctuations of the Intertropical Convergence Zone and the monsoon/ENSO/Indian Ocean dipole system influence the southern part (e.g. Saji and Yamagata 2003).

Materials and methods

Gravity core ADE3-23 was collected in 2001 during the ADIOS3 cruise of the R/V *Aegaeo*. Located SW of Crete in the Libyan Sea (Fig. 1) at 2,459 m water depth (34°750 (N, 21°880(E), the core recovered 3.49 m of grey hemipelagic mud and silty mud interlayered with three distinct, dark grey sapropelic layers (Fig. 2), defined as sapropel S1 (24–39 cm; oxidized layer 12–24 cm), S5 (225.5–236 cm) and S6 (314–326 cm) on the basis of radiochemical analyses (^{238}U, ^{234}U, ^{232}Th), and total organic carbon (TOC) and Ba contents (Fig. 2, records A, B; Gourgiotis 2003, 2004). The increase of TOC between 188 and 200 cm, together with higher values of total Ba at the same level, indicates an interval with higher productivity (Fig. 2), interpreted by Gourgiotis (2003) as a possible trace of sapropel S3 or S4.

In all, 96 samples were taken for calcareous nannofossil analysis every 3 to 5 cm in the hemipelagic mud intervals, and every 1 cm in the sapropel intervals. Sample preparation for calcareous nannofossil study followed standard smear slide techniques. Analyses were performed using a Leica DMSP polarising light microscope at 1,250× magnification by counting at least 300 specimens per sample.

Specimens resembling *Reticulofenestra* spp. are here assigned to EHMC (*E. huxleyi* moderately calcified) morphotypes, following Crudeli et al. (2004, 2006). Additional counts of 15 fields of view (Negri and Giunta 2001) were performed for the taxa *Helicosphaera* spp., *Rhabdosphaera* spp., *Syracosphaera* spp., *Coronosphaera* spp., *Calcidiscus* spp. The rare species *Braarudosphaera bigelowii* and *C. pelagicus* were counted in a fixed area of 150 fields of view. All results were converted into relative abundances (percentages) of selected species in order to avoid dilution effects, such as the input of terrigenous matter (cf. Flores et al. 1997). The calcareous nannofossil *E. huxleyi* acme zone (MNN21b, Rio et al. 1990) is defined as the interval where *E. huxleyi* frequency values exceed 20% in counts of 300 nannofossil specimens (Castradori 1993a).

A quantitative study of the planktonic foraminiferal assemblages was performed on the same samples. Each sample was washed, sieved at 150 μm and then dried at 60°C. Quantitative analysis was carried out on aliquots separated

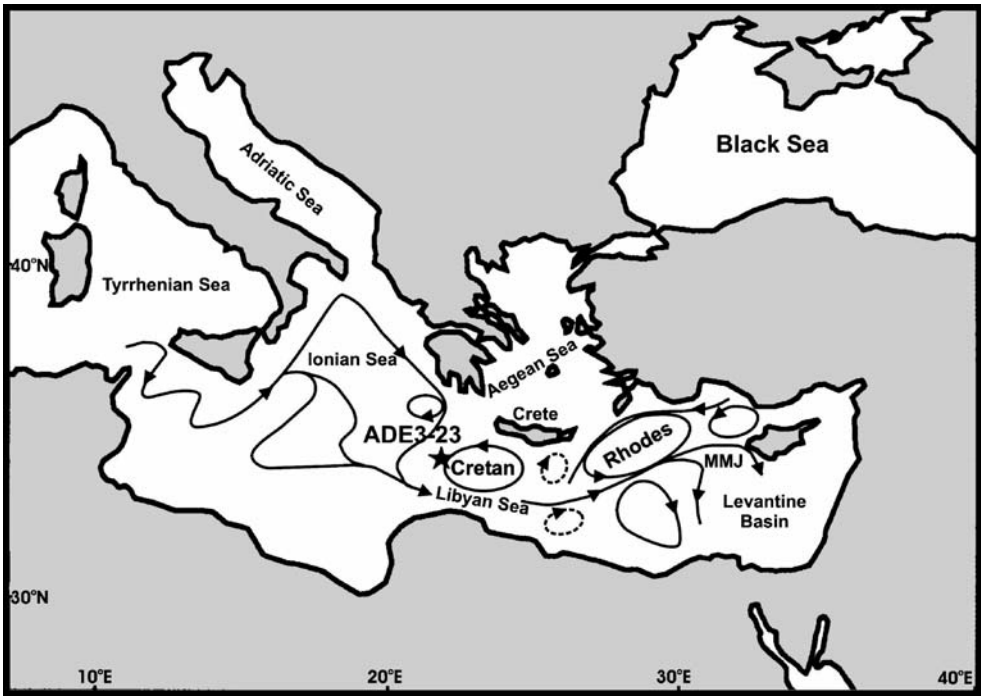

Fig. 1 Map of the Eastern Mediterranean with present-day circulation patterns (modified from Malanotte-Rizzoli et al. 1997) and location of core ADE3-23. *MMJ* Mid-Mediterranean Jet

from each sample by means of a microsplitter, in order to obtain at least 300 specimens. Planktonic foraminiferal specimens were identified and counted following the taxonomic concepts of Hemleben et al. (1989). *N. pachyderma* right and left coiling (d and s), and the two varieties of *G. ruber* (*alba* and *rosea*) were counted and plotted separately. The species *Globigerinoides sacculifer* includes also *Globigerinoides trilobus*, according to Hemleben et al. (1989); the species

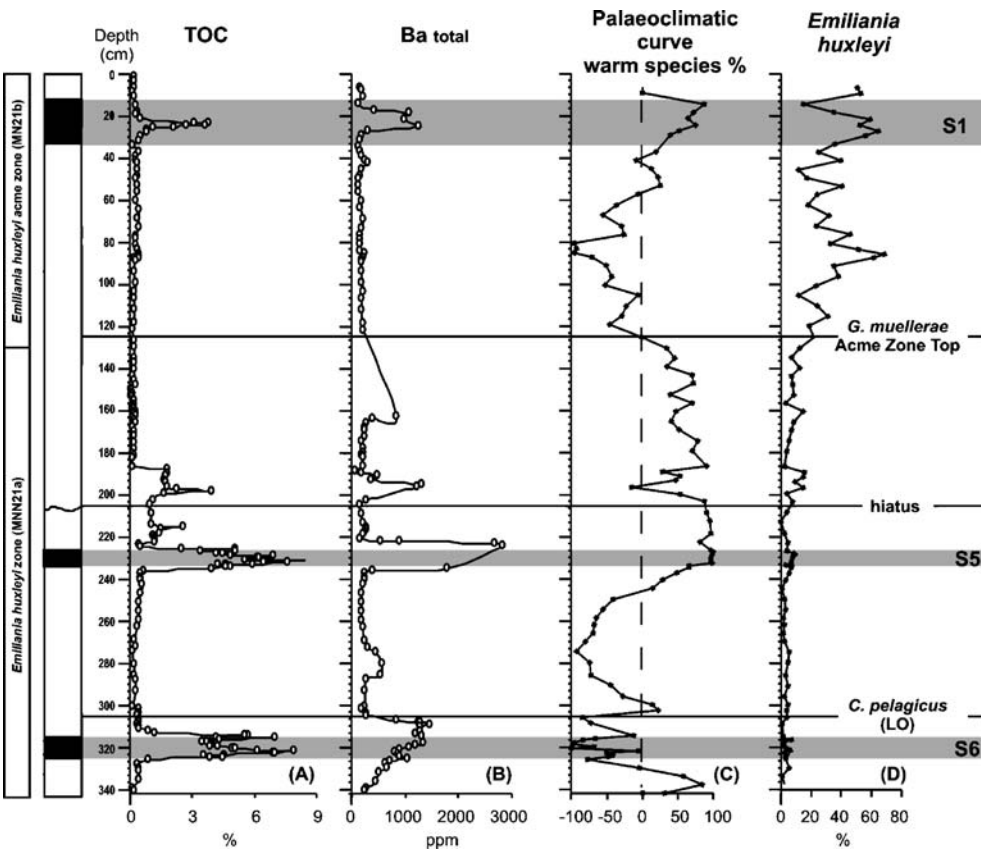

Fig. 2 Core ADE3-23 stratigraphy. *A*, *B* TOC and Ba_{total} contents (extracted from Gourgiotis 2004). *C*, *D* Palaeoclimatic curve inferred from planktonic foraminifers and relative abundance of *E. huxleyi* (present study). Calcareous nannofossil biozones are after Rio et al. (1990)

G. rubescens and *Globoturborotalita tenella* were counted and plotted together because of the similarity of their ecological characteristics (Capotondi et al. 1999). Identified species are expressed as percentages of the total number of planktonic foraminifers.

A palaeoclimatic curve, indicative of sea surface temperature (SST), is based on the planktonic foraminiferal assemblages of core ADE3-23 (Fig. 2, record C) and was obtained using the formula $(w-c)/(w+c)\times 100$ (Rohling et al. 1993), where w represents the warm-water and c the cold-water species. According to the available literature on the ecological features of planktonic Foraminifera (Bé and Tolderlund 1971; Thunell and Reynolds 1984; Hemleben et al. 1989; Rohling et al. 1993; Pujol and Vergnaud Grazzini 1995), *G. trilobus*, *G. ruber* var. *alba* and *rosea*, *G. rubescens*, *G. truncatulinoides*, *Orbulina universa* and *G. siphonifera* are considered warm-water species, whereas *Globorotalia scitula*, *G. inflata*, *T. quinqueloba* and *G. glutinata* are considered cold-water indicators.

Multivariate statistical analyses (R-mode hierarchical cluster analysis, HCA; principal component analysis, PCA) were performed on both calcareous nannofossil and planktonic foraminiferal assemblages determined in core ADE3-23, using SPSS (version 10.1) statistical software.

Age assessment

Our analysis of *E. huxleyi* specimens in core ADE3-23 (Fig. 2, record D, Fig. 3) enabled the identification of an MNN21b nannofossil biozone extending from the core top to 130 cm depth, suggesting an age younger than 52 ka (Table 1) for this part of the core. The top of the *Gephyrocapsa muellerae* acme zone at 45.7 ka (Fig. 2, Table 1), characterised by a dramatic and continuous reduction in *G. muellerae* (Fig. 3a), is recognised at 125 cm from the core top. In addition, we recorded the last occurrence (LO) of *C. pelagicus* (150–200 ka B.P., Raffi and Rio 1980) at 305 cm from the core top (Fig. 2). We used the best regression model for all the dating points (Table 1), applying cubic fitting, in order to obtain the age–depth profile for core ADE3-23. The adopted age model is further confirmed by the positions of marine isotope stages (MISs) 1–6 in the core (Fig. 3; ages used for MISs are after Martinson et al. 1987). According to our age model, the core depth of 203.5 cm from the core top has an age of ~83 ka. Therefore, our stratigraphic data reveal the imprint of sapropel S3 (midpoint age 81 ka B.P.; Lourens 2004) between 188 and 200 cm, and indicate a hiatus of approx. 35 ka between 203.5 cm (~83 ka) and 208.5 cm (~118 ka) in the core (Fig. 3). All ages used are expressed in conventional radiocarbon years.

Results

Calcareous nannofossils

Calcareous nannofossils are generally well-preserved in all samples. The most abundant species are plotted vs. age in Fig. 3a. Within MIS 1 and MIS 2, *E. huxleyi* abundances increase abruptly. The species displays values well below 20% during MIS 4–MIS 6, slightly exceeding 10% only during the deposition of S5. EHMC morphotypes are particularly evident during MIS 2. *F. profunda* shows an overall inverse distribution pattern to that of *E. huxleyi*, with highest abundance during MIS 5 (sapropel S5 depositional interval). *G. muellerae* and *Rhabdosphaera* spp. display distinctly high frequencies within MIS 3 and MIS 4, featuring also the depositional interval independently identified for sapropel S3. *Gephyrocapsa oceanica* and small *Gephyrocapsa* spp. occur mainly in MISs 5 and 6. *Coronosphaera* spp., *Helicosphaera* spp. and *Calcidiscus* spp. are overall increased within MIS 6. *Syracosphaera* spp. present the highest abundance within MIS 3 and MIS 6, particularly during the deposition of S6. *B. bigelowii* is restricted to a few levels within S1, and in S3, S5 and S6, but in very low numbers. *C. pelagicus* is represented by specimens >10 μm in the lower part of the core, mainly during the S6 depositional interval. Abundances of reworked specimens fluctuate along the core, with a major peak in MIS 2.

Planktonic foraminifers

The planktonic foraminiferal assemblage is very abundant and can be well documented (Fig. 3b). One of the most abundant species throughout the core is *G. ruber* (var. *alba* and *rosea*). *G. ruber* var. *alba* shows high relative frequencies, whereas *G. ruber* var. *rosea* is present in low percentages. *O. universa* and *G. siphonifera* generally have low and discontinuous distributions, whereas *G. rubescens* often occurs in high abundances (>20%) with sharp increases (>50%) in MISs 1, 4 and 5. *G. trilobus* is essentially confined to two significant peaks in abundance, during MIS 1 and MIS 5 (sapropel S1 and S5 depositional intervals). *G. bulloides* is abundant in the core, with a mean percentage of 25% and maximum abundance (~50%) within S6. *G. inflata* varies between 0–16%, featuring also the S3 depositional interval, but it is absent during MIS 2 and MIS 5. *G. truncatulinoides* presents notable abundances within MISs 1, 4 and 6. Peaks of *G. scitula* are significant at the base of MIS 1 and MIS 2. *G. scitula* abundance increases also during MIS 6, while *T. quinqueloba* together with *N. pachyderma* and *N. dutertrei* are the main faunal components, particularly during the sapropel S6 depositional interval.

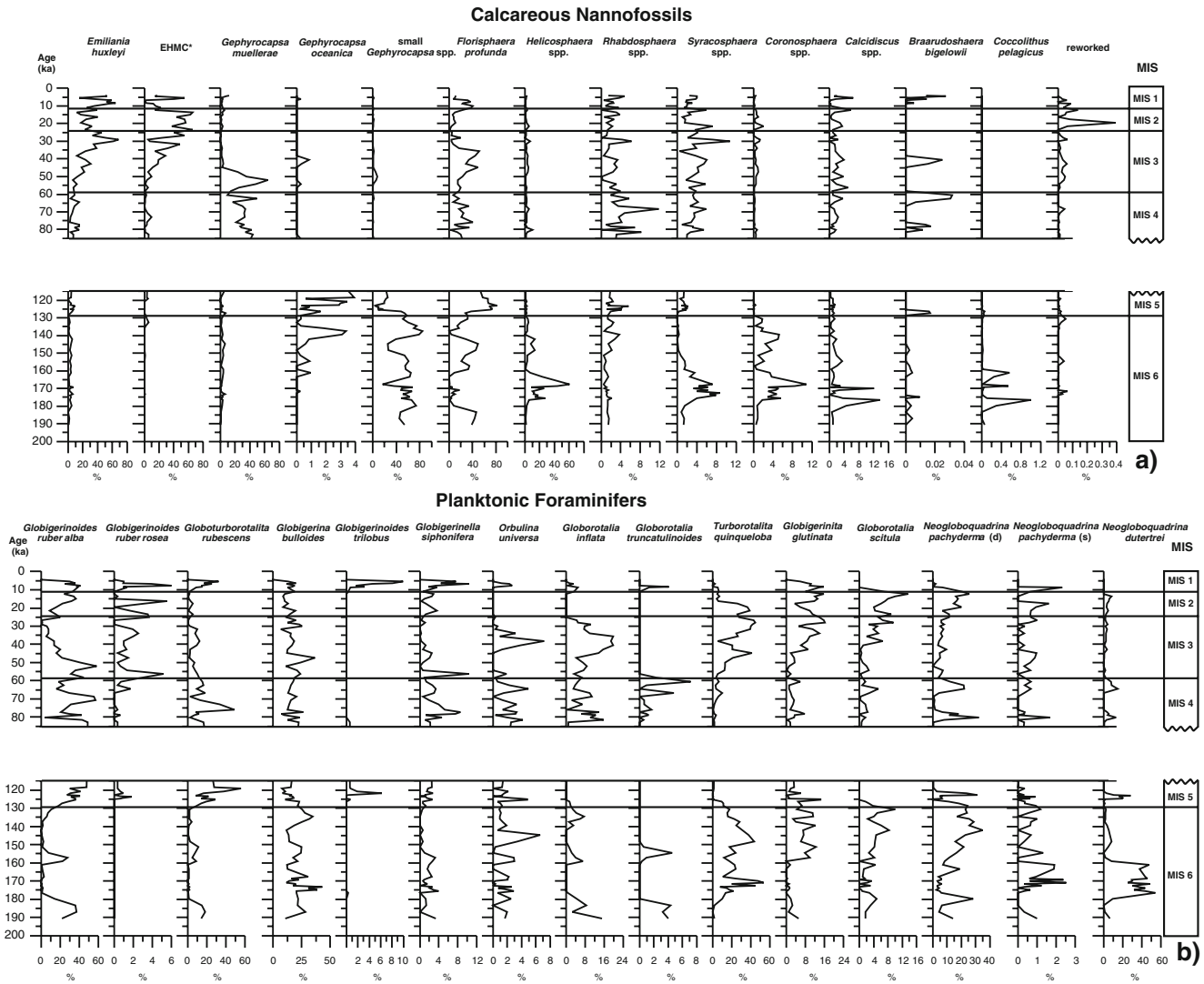

Fig. 3 Relative abundances of calcareous nannofossil (**a**) and planktonic foraminiferal species (**b**) in core ADE3-23, correlated with age (ka) and (*right*, *MIS*) the marine isotope stages. *EHMC* denotes *Emiliania huxleyi* moderately calcified morphotypes sensu Crudeli et al. (2004, 2006)

Multivariate analyses

R-mode HCA (Fig. 4a, b) of calcareous nannofossil and planktonic foraminiferal associations within the sapropels reveals two main groups, A and B (subgroups B1, B2) in each case. Among the calcareous nannofossils, group A consists of *Coronosphaera* spp., *Helicosphaera* spp., small *Gephyrocapsa* spp., *Syracosphaera* spp., *Calcidiscus* spp. and *C. pelagicus*. Group B represents a separated species (*E. huxleyi*), whereas group B2 includes *F. profunda*, *Rhabdosphaera* spp., *G. oceanica.* Among the planktonic foraminifers, group A consists of *N. dutertrei*, *G. bulloides*, *T. quinqueloba*, *G. scitula*, *N. pachyderma*. Group B comprises two smaller groups: group B1 consists of *G. glutinata*, *G. trilobus*, *G. siphonifera*, *G. truncatulinoides* and *G. inflata*; group B2 clusters *G. rubescens* and *G. ruber*.

A PCA plot reveals a distinct calcareous nannofossil/planktonic foraminifer association for each sapropel layer (Fig. 4c). Component 1 (36.4% variance; Fig. 4c) is positively loaded mainly by the planktonic foraminifer *T.*

Table 1 Age model pointers for core ADE3-23. All ages are expressed in conventional radiocarbon years

Event	Depth (cm)	Age (ka B.P.)	References
S1 midpoint	26	8.5	Lourens (2004)
G. muellerae acme zone top	125.5	45.7	Incarbona (2007)
Base *E. huxleyi* acme zone (NN21b)	130.5	52	Lourens (2004)
S5 midpoint	231	124	Lourens (2004)
S6 midpoint	320.5	172	Lourens (2004)

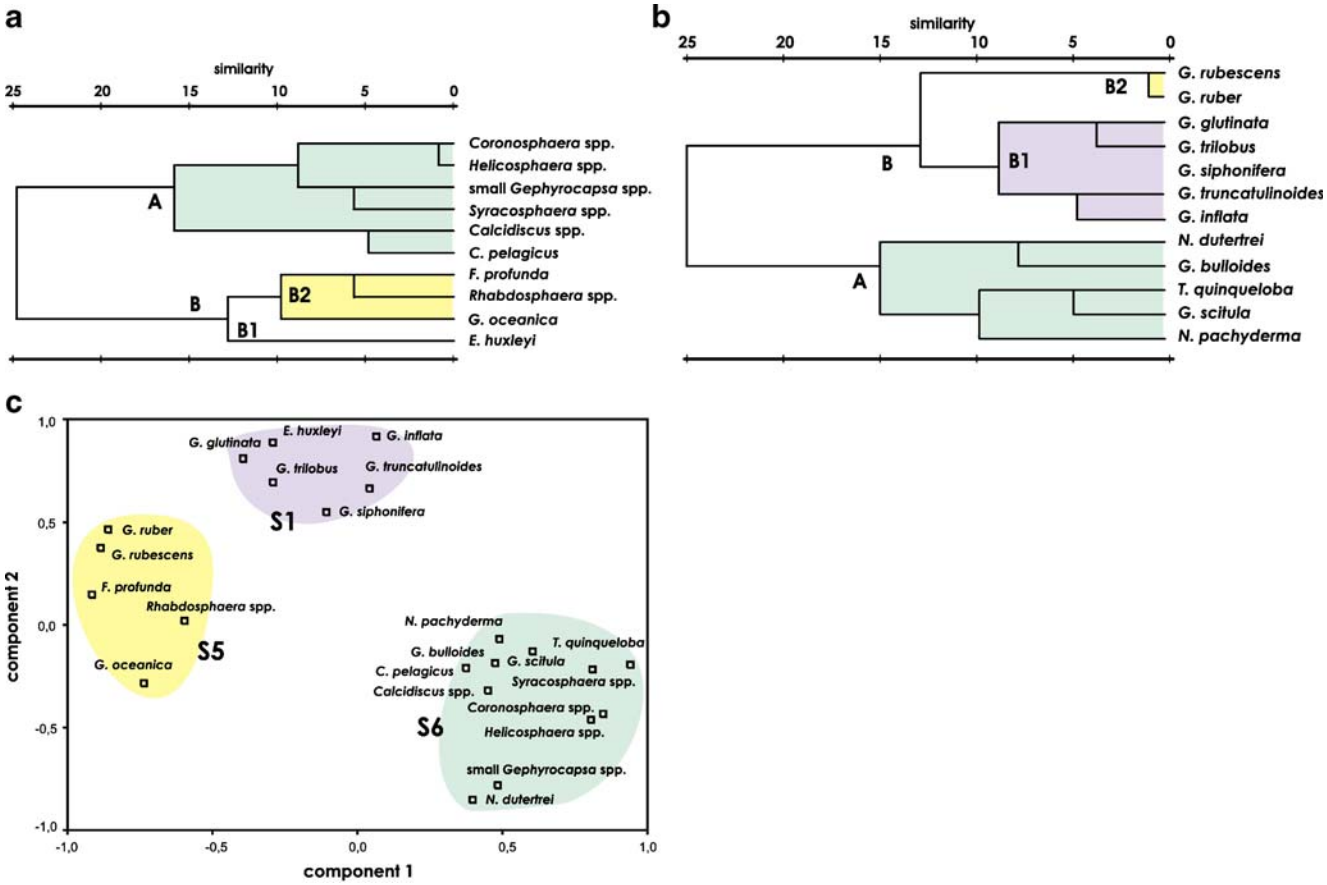

Fig. 4 Dendrograms resulting from R-mode hierarchical cluster analysis (centroid linkage method, distance metric is 1-Pearson correlation coefficient) of calcareous nannofossil (**a**) and planktonic foraminiferal (**b**) assemblages within sapropels S6, S5 and S1. **c** Biplot of two PCA components defining the ecological affinities of plankton assemblages within sapropels S6, S5 and S1

quinqueloba (0.91) and the calcareous nannofossils *Coronosphaera* spp. (0.85), *Syracosphaera* spp. (0.84) and *Helicosphaera* spp. (0.81). Component 1 is negatively loaded by the calcareous nannofossil *F. profunda* (−0.89) and the planktonic foraminifers *G. rubescens* (−0.83) and *G. ruber* (−0.82). Component 2 (26.8% variance; Fig. 4c) is positively loaded mainly by *E. huxleyi* (0.85) and *G. glutinata* (0.84), with negative loadings for *N. dutertrei* (−0.85) and small *Gephyrocapsa* spp. (−0.77).

Discussion and conclusions

Sapropel S6 depositional interval

The interval below sapropel S6 in the Libyan Sea is characterised by high SSTs, as shown in the palaeoclimatic curve (Fig. 2, record C). Relatively stratified conditions are evidenced by the presence of *F. profunda* in the calcareous nannofossil assemblages (Fig. 5a), this being a lower photic zone species of tropical and subtropical oceans (Okada and Honjo 1973) indicating the nutricline–thermocline level (Molfino and McIntyre 1990; Castradori 1993b; Incarbona et al. 2008a, 2008b). In addition, the warm-water planktonic foraminifers *G. ruber*, *G. siphonifera* and *G. rubescens* are significant components of the assemblages (Fig. 5b), justifying the interpretation of stratification in the water column (Bé and Tolderlund 1971; Fairbanks et al. 1982; Hemleben et al. 1989). However, the increases in small *Gephyrocapsa* spp., indicating higher surface productivity (Colmenero-Hidalgo et al. 2004), and of the cold-water planktonic foraminiferal species *T. quinqueloba*, *G. inflata*, *G. scitula*, *G. glutinata* and *N. pachyderma* (Geraga et al. 2005) suggest the onset of deep winter convection (Casford et al. 2003). This is consistent with the increased occurrence of *C. pelagicus* in the same interval, a species generally considered as a cold-water indicator which can also be influenced by nutrient availability (Young 1994; Cachão and Moita 2000).

Sapropel S6 represents an interval of high insolation during the early part of the penultimate glaciation (Emeis et al. 2000b), marked by high TOC and total Ba values (Fig. 2, records A, B). The planktonic foraminiferal assemblage in the lower part of S6 is characterised by the

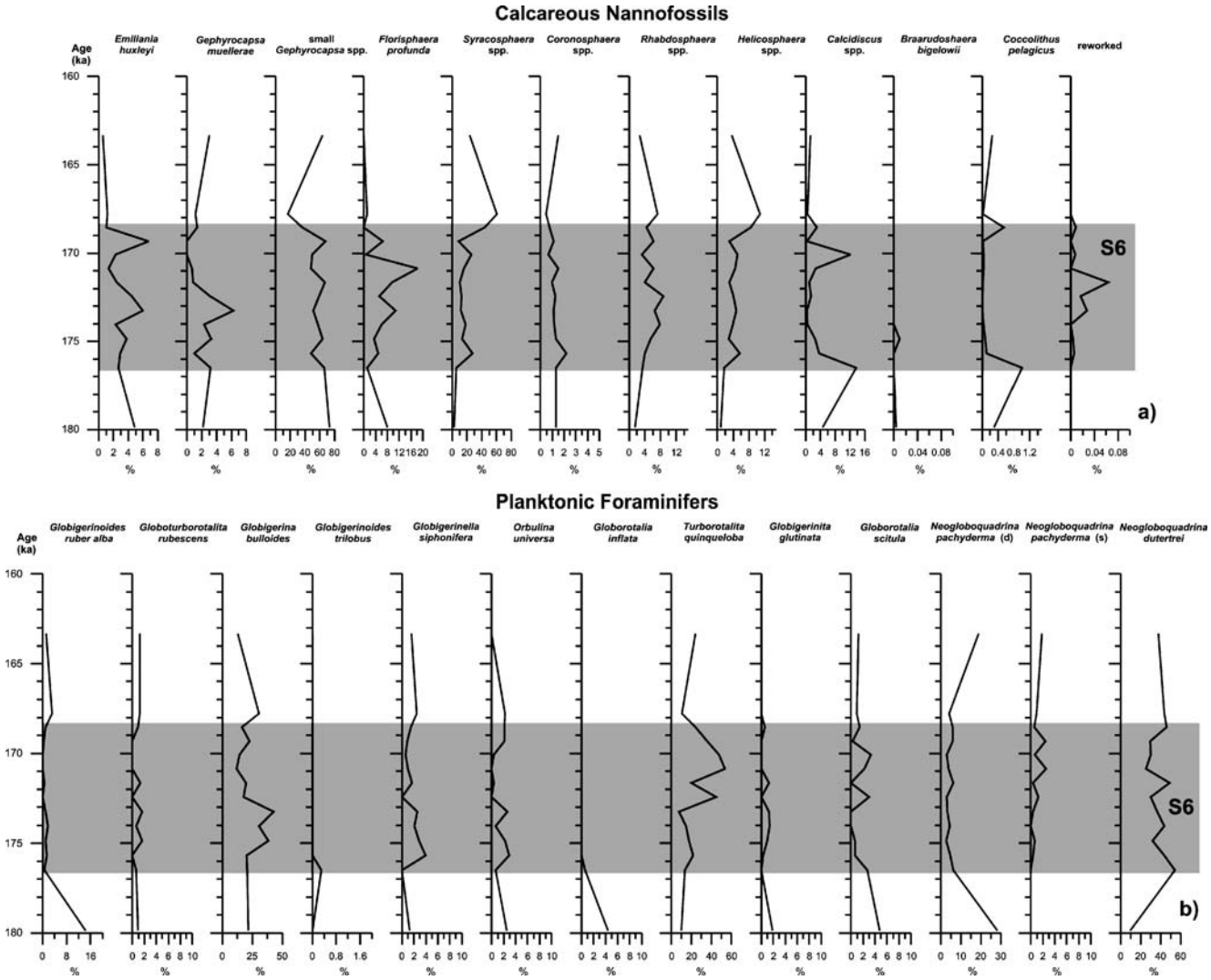

Fig. 5 Sapropel S6, core ADE3-23: distributions of selected **a** calcareous nannofossils and **b** planktonic foraminiferal species vs. age (ka)

dominance of cool-water indicators (Fig. 5b) such as *N. dutertrei*, which can also be related to high nutrient content (Toledo et al. 2007), and *G. bulloides*, a species often used as high-productivity proxy (e.g. Thiede 1983). The peaks of *C. pelagicus* and the cold-water nannofossil indicator *G. muellerae* (Samtleben et al. 1995) also reflect the prevailing very cold climatic conditions. The increase in productivity is recorded in the nannofossils by the high abundance of the small *Gephyrocapsa* spp. and *Helicosphaera* spp. (Ziveri et al. 2004; Crudeli et al. 2006). However, the absence of *C. pelagicus* in the middle part of S6, together with slight peaks of *G. siphonifera* and *O. universa*, suggests slightly warmer climatic shifts within this cold period (Fig. 5b), associated with less saline waters as documented by the distribution of *T. quinqueloba* (Rohling et al. 1997), as well as *Syracosphaera* spp. and *Helicosphaera* spp. (Flores et al. 1997; Colmenero-Hidalgo et al. 2004). The observed peak of reworked nannofossil species (Fig. 5a) may reflect higher riverine input contributing to the formation of lower-salinity surface waters. In addition, the slight increase in the DCM (deep chlorophyll maximum) dweller *N. pachyderma* sinistral (Capotondi et al. 2006), and the turnover between the stratification proxy *F. profunda* and the cold-water proxy *C. pelagicus* possibly suggest the development of a faint, temporary DCM which defines the mid S6 in the Libyan Sea. A similar observation concerning the documentation of ephemeral higher production of *F. profunda* within S6 has also been evidenced at several locations in the Eastern Mediterranean by Castradori (1993b).

The top of S6 is marked by a return to cold conditions, resulting in a mixed and more productive water column. This is suggested by the absence of *F. profunda* and the high abundance of *Helicosphaera* spp. (Fig. 5a), as well as *N. dutertrei*, *G. bulloides* and *T. quinqueloba* (Fig. 5b).

After the deposition of S6, the palaeoclimatic curve (Fig. 2, record C) suggests a prolongation of cold and

highly productive conditions in the Libyan Sea. High abundances of small *Gephyrocapsa* spp., *Coronosphaera* spp. and *N. pachyderma* mark the assemblages (Fig. 5a, b).

Sapropel S5 depositional interval

Prior to the deposition of S5 in the Libyan Sea, small *Gephyrocapsa* spp., *T. quinqueloba* and *G. scitula* prevail in the calcareous plankton assemblages, suggesting a highly productive and cool interval. However, the increasing abundance of the deep dweller *F. profunda*, together with the oligotrophic *Rhabdosphaera* spp. (Winter et al. 1994), and the planktonic foraminifers *G. ruber* and *G. rubescens* indicates the establishment of less cold and stratified conditions immediately before the deposition of S5 (Fig. 6a, b).

The lower part of S5 is characterised by very high abundance of the nutricline proxy nannofossil species *F. profunda* (Fig. 6a), suggesting particularly strong stratification in the upper photic zone and the establishment of a DCM. Higher water-column temperatures are clearly supported by the palaeoclimatic curve (Fig. 2, record C) and the abundance of warm-water planktonic foraminifers (Fig. 6b) such as *G. rubescens*, *G. siphonifera* and *O. universa*, as well as *G. ruber* (Hemleben et al. 1989). Increased runoff is also evidenced by the presence of *G. trilobus* and *N. pachyderma* (Capotondi et al. 2006). However, the co-occurrence of *G. ruber* with the chlorophyll maximum proxy *N. dutertrei* (Thunell and Sautter 1992) does not support extreme oligotrophy during this interval in the Libyan Sea, in contrast to what has been suggested by Corselli et al. (2002) for the Urania Basin northwest of our study area. Moreover, the increase in abundance of *E. huxleyi* (Fig. 6a), although never reaching 20% like previously reported (e.g. Violanti et al. 1991; Castradori 1993a; Corselli et al. 2002), suggests higher fertility in the surface waters. This event, distinctly recognised in our core from the Libyan Sea, most likely corresponds

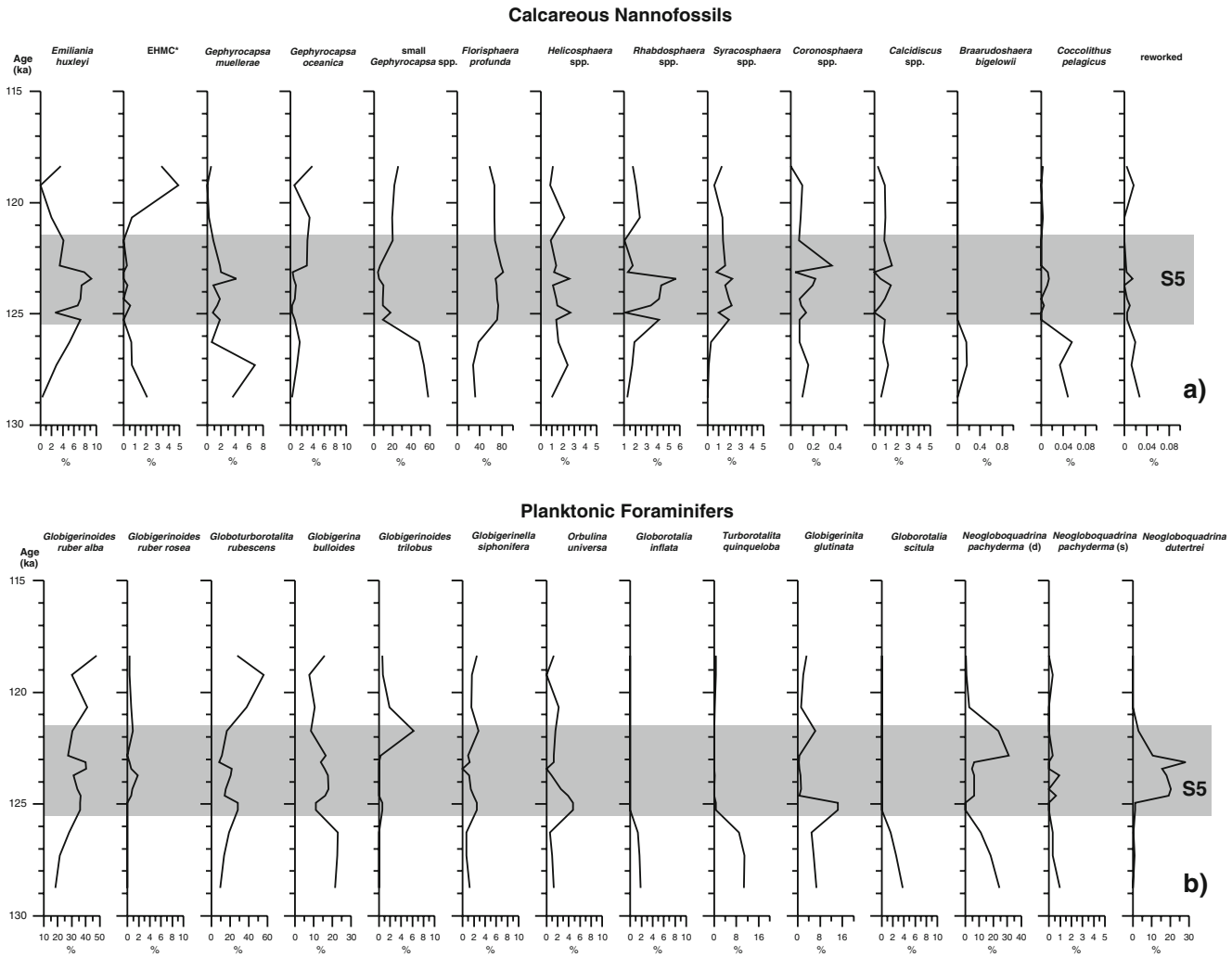

Fig. 6 Sapropel S5, core ADE3-23: distributions of selected **a** calcareous nannofossils and **b** planktonic foraminiferal species vs. age (ka)

to the timing of relaxation in the northward penetration of the African monsoon and the concomitant strong high-latitude circulation already recorded within S5 in the South-Eastern Mediterranean (Rohling et al. 2002a, 2004).

The upper part of S5 is characterised by a turnover between increased *G. oceanica* and small *Gephyrocapsa* spp., and reduced values of *Rhabdosphaera* spp. (Fig. 6a). The presence of the former species suggests higher surface-water temperatures (Winter et al. 1994) but is also related with less saline waters (Knappertsbusch 1993). At the same level in the core, *F. profunda* (although dominating the assemblages) starts to decrease, similarly to what has been observed at other Eastern Mediterranean locations (Corselli et al. 2002; Giunta et al. 2006). Together with the turnover between *G. ruber* and *N. pachyderma* dextral, this suggests a breakdown of stratification towards the top of S5 in the Libyan Sea.

Above S5, increases in *E. huxleyi* moderately calcified morphotypes, which are restricted to cool Holocene intervals (Crudeli et al. 2004), and in dextral neogloboquadrinid forms, together with high values of small *Gephyrocapsa* spp. and *G. oceanica*, indicate cooler surface temperatures related with fresh-water input. However, the relatively high frequencies of *F. profunda*, *G. ruber*, *G. rubescens* and *G. trilobus* (Fig. 3) imply the continuation of deep photic zone productivity in the Libyan Sea, contrasting with what has been previously observed in the Urania Basin (Corselli et al. 2002).

Sapropel S1 depositional interval

High abundances of EHMC morphotypes and of the planktonic foraminifers *G. glutinata*, *T. quinqueloba*, *G. scitula* and *N. pachyderma* (Fig. 3) point to generally cold and highly fertile surface waters at the base of the Holocene in the Libyan Sea. However, the increase in *Helicosphaera* spp. confirms higher fresh-water input prior to the S1 depositional interval (Fig. 7a), similarly to observations from the Aegean Sea (Triantaphyllou et al. 2009). In addition, the concomitant gradual increase in the nutricline

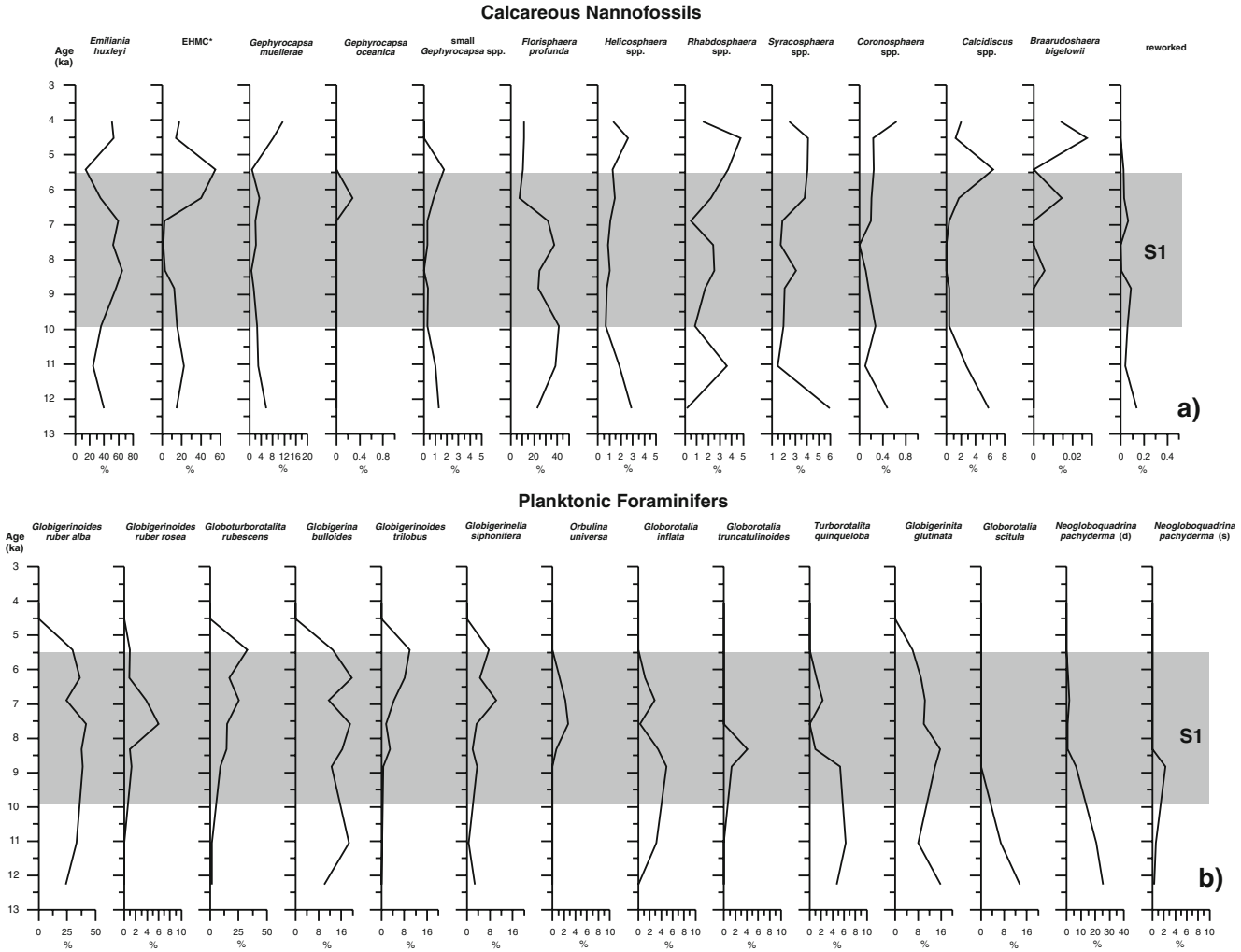

Fig. 7 Sapropel S1, core ADE3-23: distributions of selected **a** calcareous nannofossils and **b** planktonic foraminiferal species vs. age (ka)

proxy *F. profunda* (Fig. 7a) and the warm planktonic foraminifer *G. ruber* (Fig. 7b) supports the establishment of stratified conditions and the onset of a nutrient-rich environmental regime in the deep photic zone.

The lower part of S1 is characterised by increased abundance of *F. profunda*, *Helicosphaera* spp., *G. glutinata* and *G. bulloides* (Fig. 7a, b), indicating high productivity mainly in the deeper part of the water column. The relatively high values of the warm-water species *G. ruber* imply higher SSTs in the upper photic zone, as previously inferred by Negri and Giunta (2001), Principato et al. (2006) and Triantaphyllou et al. (2009) in other parts of the Eastern Mediterranean.

At ~8 ka there is a clear reduction in *F. profunda* abundance, associated with an increase in the high-nutrient indicator *E. huxleyi* (Young 1994) and the deep winter convection proxies *G. inflata* and *G. truncatulinoides* (Fig. 7a, b). Therefore, this level in the core can be roughly associated with a temporary decline of stratified conditions mirroring the S1 interruption interval, already recognised at several Eastern Mediterranean locations (e.g. De Rijk et al. 1999; Geraga et al. 2000; Triantaphyllou et al. 2009) and correlating mostly with a weakening in the African monsoon intensity and an intensified impact of harsher, higher-latitude climate conditions in the Mediterranean region (Rohling et al. 2002a, 2002b, 2004). The upper part of S1 in the Libyan Sea is characterised by a turnover between increased EHMC morphotypes and reduced *F. profunda* (Fig. 7a), pointing to high productivity in the upper photic zone. The decrease in *F. profunda*, associated with peaks in *B. bigelowii* and *G. trilobus* towards the top of S1, has already been documented by Negri and Giunta (2001), Principato et al. (2006) and Triantaphyllou et al. (2009) in the Ionian and Aegean seas, implying increased runoff and a concomitant break in stratification.

Ecological affinities of plankton assemblages within sapropels S6, S5 and S1

The multivariate analysis performed in this study suggests that component 1 reflects decreasing temperature and stratification conditions in the water column, as it is highly correlated with calcareous nannofossils and planktonic foraminiferal indicators of low temperature–high surface productivity (Fig. 4c). Therefore, members of this association (group A in HCA, Fig. 4a, b) are considered to have similar ecological affinities, and prove to be typical for sapropel S6 in the Libyan Sea. Component 2 (Fig. 4c) probably reflects the degree of fresh-water input in the middle–upper photic zone. This factor is negatively correlated with the attributes of the S6 assemblage. Surface-water temperature reconstructions in the Eastern Mediterranean Sea (Emeis et al. 2000a) and palynological investigations (e.g. Rossignol-Strick and Paterne 1999) indicate a cool and arid climate during the deposition of S6. These conditions have resulted in denser surface water (Emeis et al. 2003) and higher salinities. Together with wind-induced mixing, this may have prevented both permanent water-column stratification and permanent anoxia at the seafloor, although the presence of a faint deep chlorophyll maximum detected in our Libyan Sea record in the middle part of sapropel S6 suggests a temporary climatic amelioration.

The high temperature and stratification indicators of group B2 in HCA (Fig. 4a, b) are negatively correlated with component 1, featuring the strongly stratified and warm conditions within sapropel S5. Component 2 is moderately correlated with the S5 assemblage. Strong runoff from the Nile and other rivers in our study area seems unlikely (Weldeab et al. 2003; Giunta et al. 2006; Sangiorgi et al. 2006). In particular, Weldeab et al. (2003) examined whether riverine nutrients were the main cause for the high export production during S5, and suggested a southward shift of the Cretan gyre within the framework of an Eemian weak anti-estuarine circulation system (e.g. Stratford et al. 2000). However, pulses of fresh-water input during S5 have been evidenced in our record by the presence of *G. oceanica*. Together with *F. profunda* reduction, this can be associated with a shift to colder climatic conditions, resulting in the breakdown of stratification recorded towards the top of S5.

The assemblage of the high productivity–deep convective mixing group B1 in HCA (Fig. 4a, b) presents moderate correlation with component 1 and is associated with sapropel S1. The assemblage of S1 is positively correlated with component 2, indicating higher inputs of fresh water during its formation. Emeis et al. (2000a) have demonstrated that homogeneity in surface-water salinity in the Eastern Mediterranean during S1 is consistent with multiple fresh-water sources channelled not solely by the Nile watershed, as has been proven by examining fossil river systems in North Africa (Gasse 2000). The presence of *G. trilobus* in S1 assemblages (Fig. 4b) reinforces the interpretation of increased runoff. In addition, *G. inflata*, *G. truncatulinoides* and *E. huxleyi* imply high productivity in the middle–upper water column, strongly associated with weak stratification and moderate sea surface temperatures which reflect a more variable climate (e.g. Gogou et al. 2007; Triantaphyllou et al. 2009) during S1 times.

In conclusion, our study has identified the plankton assemblages—both calcareous nannofossils and planktonic foraminifers—which typify the sapropels S6, S5 and S1 in the Libyan Sea. This has enabled the establishment of ecological affinities within and between the different sapropel layers and, thereby, the detection of climatic variability impacts during their deposition in this part of

the Eastern Mediterranean. The findings that a warmer interval is recognised in the middle part of the cold S6, enhanced surface productivity and breakdown of stratification are observed in the middle–upper part of the warm S5, and weak stratification is recorded in the upper S1 contribute to the mounting body of evidence that climate variability was more pronounced than commonly considered to date for these Eastern Mediterranean sapropel depositional intervals.

Acknowledgements The valuable suggestions of Jeremy Young, Jose-Abel Flores and Maria Bianca Cita on earlier versions of the manuscript have significantly upgraded this study. Critical comments by two anonymous referees and the journal editors have proved useful in improving the manuscript. Thanks are due to A. Gourgiotis for providing us data on core ADE3-23. Financial support through University of Athens Research Projects 70/4/8644 to M. Triantaphyllou and 70/4/8642 to A. Antonarakou is greatly acknowledged. C. Sepetzoglou, T. Tsourou and G. Kontakiotis are warmly thanked for kind assistance during the analyses.

References

Bé AWH, Tolderlund DS (1971) Distribution and ecology of living planktonic foraminifera in surface waters of the Atlantic and Indian Oceans. In: Funnell BM, Riedel WR (eds) Micropaleontology of the oceans. Cambridge University Press, Cambridge, pp 105–150

Bethoux JP, Gentili B, Morin P, Nicolas E, Pierre C, Ruiz-Pino D (1999) The Mediterranean Sea: a miniature ocean for climatic and environmental studies and a key for the climatic functioning of the North Atlantic. Prog Oceanogr 44:131–146

Cachão M, Moita MT (2000) *Coccolithus pelagicus*, as a productivity proxy related to moderate fronts off Western Iberia. Mar Micropaleontol 39:131–155

Cane T, Rohling EJ, Kemp AES, Cooke S, Pearce RB (2002) High-resolution stratigraphic framework for Mediterranean sapropel S5: defining temporal relationships between records of Eemian climate variability. Palaeogeogr Palaeoclimatol Palaeoecol 183:87–101

Capotondi L, Borsetti A, Morigi C (1999) Foraminiferal ecozones, a high resolution proxy for the late Quaternary biochronology in the central Mediterranean Sea. Mar Geol 153:253–274

Capotondi L, Principato MS, Morigi C, Sangiorgi F, Maffioli P, Giunta S, Negri A, Corselli C (2006) Foraminiferal variations and stratigraphic implications to the deposition of sapropel S5 in the Eastern Mediterranean. Palaeogeogr Palaeoclimatol Palaeoecol 235:48–65

Casford JSL, Rohling EJ, Abu-Zied RH, Fontanier C, Jorissen FJ, Leng MJ, Schmiedl G, Thomson J (2003) A dynamic concept for Eastern Mediterranean circulation and oxygenation during sapropel formation. Palaeogeogr Palaeoclimatol Palaeoecol 190:103–119

Castradori D (1993a) Calcareous nannofossil biostratigraphy and biochronology in Eastern Mediterranean deep-sea cores. Riv Ital Paleontol Stratigr 99:107–126

Castradori D (1993b) Calcareous nannofossil and the origin of Eastern Mediterranean sapropels. Paleoceanography 8:459–471

Cita MB, Vergnaud Grazzini C, Robert C, Chamley H, Ciaranfi N, d'Onofrio S (1977) Paleoclimatic record of a long deep sea core from the Eastern Mediterranean. Quat Res 8:205–235

Colmenero-Hidalgo E, Flores JA, Sierro FJ, Bárcena MÁ, Löwemark L, Schönfeld J, Grimalt JO (2004) Ocean surface water response to short-term climate changes revealed by coccolithophores from the Gulf of Cadiz (NE Atlantic) and Alboran Sea (W Mediterranean). Palaeogeogr Palaeoclimatol Palaeoecol 205:317–336

Corselli C, Principato MS, Maffioli P, Crudeli D (2002) Changes in planktonic assemblages during sapropel S5 deposition: evidence from Urania Basin area, Eastern Mediterranean. Paleoceanography 17(3):1–30. doi:10.1029/2000PA000536

Crudeli D, Young JR, Erba E, de Lange GJ, Henriksen K, Kinkel H, Slomp CP, Ziveri P (2004) Abnormal carbonate diagenesis in Holocene–late Pleistocene sapropel-associated sediments from the Eastern Mediterranean; evidence from *Emiliania huxleyi* coccolith morphology. Mar Micropaleontol 52:217–240

Crudeli D, Yong JR, Erba E, Geisen M, Ziveri P, de Lange GJ, Slomp CP (2006) Fossil record of holococcoliths and selected hetero-holococcolith associations from the Mediterranean (Holocene–late Pleistocene): evaluation of carbonate diagenesis and palaeoecological–palaeoceanographic implications. Palaeogeogr Palaeoclimatol Palaeoecol 237:191–212

de Lange GJ, van Santvoort PJM, Langereis C, Thomson J, Corselli C, Michard A, Rossignol-Strick M, Paterne M, Anastasakis G (1999) Palaeo-environmental variations in Eastern Mediterranean sediments: a multidisciplinary approach in a prehistoric setting. Prog Oceanogr 44:369–386

De Rijk S, Hayes A, Rohling EJ (1999) Eastern Mediterranean sapropel S1 interruption: an expression of the onset of climatic deterioration around 7 ka BP. Mar Geol 153:337–343

Emeis KC, Struck U, Schulz HM, Rosenberg R, Bernasconi S, Erlenkeuser H, Sakamoto T, Martinez-Ruiz F (2000a) Temperature and salinity variations of Mediterranean Sea surface waters over the last 16, 000 years from records of planktonic stable oxygen isotopes and alkenone unsaturation ratios. Palaeogeogr Palaeoclimatol Palaeoecol 158:259–280

Emeis KC, Sakamoto T, Wehausen R, Brumsack HJ (2000b) The sapropel record of the Eastern Mediterranean Sea—results of Ocean Drilling Program Leg 160. Palaeogeogr Palaeoclimatol Palaeoecol 158:371–395

Emeis KC, Schultz HM, Struck U, Rossignol-Strick M, Erlenkeusen H, Howell M, Kroon D, Mackensen A, Ishizuka S, Oba T, Sakamoto T, Koizumi I (2003) Eastern Mediterranean surface water temperatures and $\delta^{18}O$ composition during deposition of sapropels in the late Quaternary. Paleoceanography 18(1):1–18

Fairbanks RG, Sverdlove M, Free R, Wiebe PH, Bé AWH (1982) Vertical distribution of living planktonic foraminifera from the Panama basin. Nature 298:841–844

Flores JA, Sierro FJ, Francés G, Vázquez A, Zamarreño I (1997) The last 100, 000 years in the western Mediterranean: sea surface water and frontal dynamics as revealed by coccolithophores. Mar Micropaleontol 29:351–366

Gasse F (2000) Hydrological changes in the African tropics since the last glacial maximum. Quat Sci Rev 19:189–211

Geraga M, St T-M, Ch I, Papatheodorou G, Ferentinos G (2000) An evaluation of paleoenvironmental changes during the last 18000 yrs BP in the Myrtoon Basin, S.W. Aegean Sea. Palaeogeogr Palaeoclimatol Palaeoecol 156:1–17

Geraga M, St T-M, Ch I, Papatheodorou G, Ferentinos G (2005) Short-term climate changes in the southern Aegean Sea over the last 48.000 years. Palaeogeogr Palaeoclimatol Palaeoecol 220:311–332

Giunta S, Negri A, Morigi C, Capotondi L, Combourieu-Nebout N, Emeis KC, Sangiorgi F, Vigliotti L (2003) Coccolithophorid ecostratigraphy and multi-proxy paleoceanographic reconstruction in the Southern Adriatic Sea during the last deglacial time (Core AD91–17). Palaeogeogr Palaeoclimatol Palaeoecol 190:39–59

Giunta S, Negri A, Maffioli P, Sangiorgi F, Capotondi L, Morigi C, Principato MS, Corselli C (2006) Phytoplankton dynamics in the

Eastern Mediterranean Sea during Marine Isotopic Stage 5e. Palaeogeogr Palaeoclimatol Palaeoecol 235(1/3):28–47

Gogou A, Bouloubassi I, Lykousis V, Arnaboldi M, Gaitani P, Meyers PA (2007) Organic geochemical evidence of abrupt late glacial-Holocene climate changes in the North Aegean Sea. Palaeogeogr Palaeoclimatol Palaeoecol 256:1–20

Gourgiotis A (2003) Sedimentology and geochemistry of recent sediments in Eastern Mediterranean. Department of Marine Sciences, University of the Aegean, Mytilene, Diploma

Gourgiotis A (2004) Etude géochimique du Sapropèle S5 de Méditerranée orientale: une approche radiochimique. Serait-il possible que les sapropèles soient des indicateurs des grands évènements sismiques? DEA Océanologie Météorologie et Environnement, Laboratoire des Sciences du Climat et de l'Environnement, CNRS-CEA, Université P. et M. Curie Paris IV

Hemleben C, Spindler M, Anderson OR (1989) Modern planktonic foraminifera. Springer, Berlin, pp 1–363

Incarbona A (2007) Paleoceanografia del Canale di Sicilia (Mediterraneo Centrale) durante gli ultimi 350 mila anni, rivelata dalle associazioni a nannofossili calcarei. PhD Thesis, Università degli Studi di Palermo, pp 1–127

Incarbona A, Bonomo S, Di Stefano E, Zgozi S, Essarbout N, Talha M, Tranchida G, Bonanno A, Patti B, Placenti F, Buscaino G, Cuttitta A, Basilone G, Bahri T, Massa F, Censi P, Mazzola S (2008a) Calcareous nannofossil surface sediment assemblages from the Sicily Channel (central Mediterranean Sea): palaeoceanographic implications. Mar Micropaleontol 67:297–309

Incarbona A, Di Stefano E, Sprovieri R, Bonomo S, Censi P, Dinarès-Turell J, Spoto S (2008b) Variability in the vertical structure of the water column and paleoproductivity reconstruction in the central-western Mediterranean during the Late Pleistocene. Mar Micropaleontol 67:26–41

Karageorgis AP, Gardner WD, Georgopoulos D, Mishonov AV, Krasakopoulou E, Anagnostou C (2008) Particle dynamics in the Eastern Mediterranean Sea: a synthesis based on light transmission, PMC, and POC archives (1991–2001). Deep-Sea Res 55:177–202

Knappertsbusch M (1993) Geographic distribution of living and Holocene coccolithophores in the Mediterranean Sea. Mar Micropaleontol 21:219–247

Lourens LJ (2004) Revised tuning of Ocean drilling Program Site 964 and KC01B (Mediterranean) and implication for the $\delta^{18}O$, tephra, calcareous nannofossil, and geomagnetic chronologies of the past 1.1 Myr. Paleoceanography 19 PA3010. doi:10.1029/2003PA000997

Lourens LJ, Hilgen FJ, Gudjonsson L, Zachariasse WJ (1992) Late Pliocene to Early Pleistocene astronomically forced sea surface productivity and temperature variations in the Mediterranean. Mar Micropaleontol 19:49–78

Malanotte-Rizzoli P, Manca BB, Ribera d'Alcalà M, Theocharis A, Bergamasco A, Bregant D, Budillon G, Civitarese G, Georgopoulos D, Michelato A, Sansone E, Scarazzato P, Souvermezoglou E (1997) A synthesis of the Ionian Sea hydrography, circulation and water mass pathways during POEM-Phase I. Prog Oceanogr 39:153–204

Marino G (2008) Paleoceanography of the interglacial Eastern Mediterranean Sea. LPP Foundation, Utrecht, Contr Ser 24

Martinson DG, Pisias NG, Hays JD, Imbrie J, Moore TC, Shackleton NJ (1987) Age dating and the orbital theory of the ice ages; development of a high resolution 0 to 300, 000-year chronostratigraphy. Quat Res 27:1–29

Molfino B, McIntyre A (1990) Precessional forcing of nutricline dynamics in the Equatorial Atlantic. Science 249:766–769

Negri A, Giunta S (2001) Calcareous nannofossil paleoecology in the sapropel S1 of the Eastern Ionian sea: paleoceanographic implications. Palaeogeogr Palaeoclimatol Palaeoecol 169:101–112

Negri A, Capotondi L, Keller J (1999) Calcareous nannofossils, planktonik foraminifera and oxygen isotopes in the late Quaternary sapropels of the Ionian Sea. Mar Geol 157:89–103

Okada H, Honjo S (1973) The distribution of ocean coccolithophorids in the Pacific. Deep-Sea Res 20:355–374

Pinardi N, Masetti E (2000) Variability of the large scale general circulation of the Mediterranean Sea from observations and modelling: a review. Palaeogeogr Palaeoclimatol Palaeoecol 158:153–173

POEM Group (1992) General circulation of the Eastern Mediterranean. Earth-Sci Rev 32:285–309

Principato M, Giunta S, Corselli C, Negri A (2003) Late Pleistocene-Holocene planktonic assemblages in three box-cores from the Mediterranean Ridge area (west-southwest of Crete): paleoecological and paleoceanographic reconstruction of sapropel S1 interval. Palaeogeogr Palaeoclimatol Palaeoecol 190:61–77

Principato M, Crudeli D, Ziveri P, Slomp CP, Corselli C, Erba E, de Lange GJ (2006) Phyto- and zooplankton paleofluxes during the deposition of sapropel S1 (Eastern Mediterranean): biogenic carbonate preservation and paleoecological implications. Palaeogeogr Palaeoclimatol Palaeoecol 235:8–27

Psarra S, Tselepides A, Ignatiades L (2000) Primary productivity in the oligotrophic Cretan Sea (NE Mediterranean): seasonal and interannual variability. Prog Oceanogr 46:187–204

Pujol C, Vergnaud Grazzini C (1995) Distribution patterns of live planktic foraminifers as relate to regional hydrography and productive systems of the Mediterranean Sea. Mar Micropaleontol 25:187–217

Raffi I, Rio D (1980) *Coccolithus pelagicus* (Wallich): a paleotemperature indicator in the Late Pliocene Mediterranean deep sea record. Quaderno 1:176–179

Rio D, Fornaciari E, Raffi I (1990) Late Oligocene through early Pleistocene calcareous nannofossils from the western equatorial Indian Ocean (Leg 115). Proc Sci Results ODP Leg 115, Mascarene Plateau. ODP, College Station, TX, pp 175–235

Rohling EJ, Gieskes WWC (1989) Late Quaternary changes in the Mediterranean intermediate water density and formation rate. Paleoceanography 4:531–545

Rohling EJ, Hilgen FJ (1991) The Eastern Mediterranean climate at times of sapropel formation: a review. Geol Mijnb 70:253–264

Rohling EJ, Jorissen FJ, Vergnaud Grazzini C, Zachariasse WJ (1993) Northern Levantine and Adriatic quaternary planktic foraminifera; reconstruction of paleoenvironmental gradients. Mar Micropaleontol 21:191–218

Rohling EJ, Jorissen FJ, de Stigter HC (1997) 200 Year interruption of Holocene sapropel formation in the Adriatic sea. J Micropaleontol 16:97–108

Rohling EJ, Cane TR, Cooke S, Sprovieri M, Bouloubassi I, Emeis KC, Schiebel R, Kroon D, Jorissen FJ, Lorre A, Kemp AES (2002a) African monsoon variability during the previous interglacial maximum. Earth Planet Sci Lett 202:61–75

Rohling EJ, Mayewski PA, Abu-Zied RH, Casford JSL, Hayes A (2002b) Holocene atmosphere–ocean interactions: records from Greenland and the Aegean Sea. Climate Dynamics 18:587–593

Rohling EJ, Sprovieri M, Cane TR, Casford JSL, Cooke S, Bouloubassi I, Emeis KC, Schiebel R, Rogerson M, Hayes A, Jorissen FJ, Kroon D (2004) Reconstructing past planktic foraminiferal habitats using stable isotope data: a case history for Mediterranean sapropel S5. Mar Micropaleontol 50:89–123

Rossignol-Strick M, Paterne M (1999) A synthetic pollen record of the Eastern Mediterranean sapropels of the last 1 Ma: implications for the time-scale and formation of sapropels. Mar Geol 153:221–237

Saji NH, Yamagata T (2003) Indian ocean dipole mode events and African rainfall variability. CLIVAR Exch 27:1–4

Samtleben C, Baumann KH, Schröder-Ritzrau A (1995) Distribution, composition and seasonal variation of coccolithophore communities in the northern North Atlantic. In: Flores JA, Sierro FJ

(eds) Proc 5th Int Nannoplankton Association Conf. Universidad de Salamanca, Salamanca, pp 219–235

Sangiorgi F, Dinelli E, Maffioli P, Capotondi L, Giunta S, Morigi C, Principato MS, Negri A, Emeis KC, Corselli C (2006) Geochemical and micropaleontological characterisation of a Mediterranean sapropel S5: a case study from core BAN89GC09 (south of Crete). Palaeogeogr Palaeoclimatol Palaeoecol 235 (1/3):192–207. doi:10.1016/j.palaeo.2005.09.029

Stratford K, Williams RG, Myers PG (2000) Impact of the circulation on sapropel formation in the Eastern Mediterranean. Global Biogeochem Cycles 14:683–695

Thiede J (1983) Skeletal plankton and nekton in upwelling water masses off northwestern South America and northwestern Africa. In: Suess E, Thiede J (eds) Coastal upwelling: its sedimentary record. Part A. Plenum Press, New York, pp 183–208

Thunell RC, Reynolds LA (1984) Sedimentation of planktonic foraminifera: seasonal changes in species flux in the Panama Basin. Micropaleontology 30(1):47–173

Thunell R, Sautter LR (1992) Planktonic foraminiferal faunal and stable isotope indices of upwelling: a sediment trap study in the San Pedro Basin, South California Bight. In: Summerhayes CP, Prell WL, Emeis KC (eds) Upwelling systems: evolution since the early Miocene. Geol Soc Spec Publ 64:77–91

Toledo FAL, Cachao M, Costa KB, Pivel AAG (2007) Planktonic foraminifera, calcareous nannoplankton and ascidian variations during the last 25 kyr in the Southwestern Atlantic: a paleoproductivity signature? Mar Micropaleontol 64:67–79

Triantaphyllou MV, Antonarakou A, Kouli K, Dimiza M, Kontakiotis G, Papanikolaou MD, Ziveri P, Mortyn PG, Lianou V, Lykousis V, Dermitzakis MD (2009) Late Glacial-Holocene ecostratigraphy of the south-eastern Aegean Sea, based on plankton and pollen assemblages. Geo Mar Lett (in press). doi:10.1007/s00367-009-0139-5

Vergnaud-Grazzini C, Ryan WBF, Cita MB (1977) Stable isotopic fractionation, climate change and episodic stagnation in the Eastern Mediterranean during the Late Quaternary. Mar Micropaleontol 2:353–370

Violanti D, Grecchi G, Castradori D (1991) Paleoenvironmental interpretation of core BAN88–11GC (Eastern Mediterranean, Pleistocene–Holocene) on the grounds of foraminifera, thecosomata and calcareous nannofossils. Quaternario 4:13–39

Weldeab S, Emeis KC, Hemleben C, Schmiedl G, Schulz H (2003) Spatial productivity variations during formation of sapropels S5 and S6 in the Mediterranean Sea: evidence from Ba contents. Palaeogeogr Palaeoclimatol Palaeoecol 191(2):169–190

Winter A, Jordan RW, Roth P (1994) Biogeography of living coccolithophores in oceanic waters. In: Winter A, Siesser WG (eds) Coccolithophores. Cambridge University Press, Cambridge, pp 13–27

Young JR (1994) Functions of coccoliths. In: Winter A, Siesser WG (eds) Coccolithophores. Cambridge University Press, Cambridge, pp 63–82

Ziveri P, Baumann KH, Böckel B, Bollmann J, Young J (2004) Biogeography of selected coccolithophorids in the Atlantic Ocean, from Holocene sediments. In: Thierstein H, Young J (eds) Coccolithophores: from molecular processes to global impact. Springer, Berlin, pp 403–428